Journal of Alloys and Compounds 521 (2012) 71–76

Contents lists available at SciVerse ScienceDirect

Journal of Alloys and Compounds

journal homepage: www.elsevier.com/locate/jallcom

Investigation of the optical properties of $Mg(OH)_2$ and MgO nanostructures obtained by microwave-assisted methods

R. Al-Gaashani[a,b,*], S. Radiman[a], Y. Al-Douri[c,**], N. Tabet[d], A.R. Daud[a]

[a] School of Applied Physics, Faculty Science and Technology, Universiti Kebangsaan Malaysia, 43600 Bangi, Selangor, Malaysia
[b] Department of Physics, Faculty of Applied Sciences, Thamar University, Dhamar, Republic of Yemen
[c] Institute of Nano Electronic Engineering, University Malaysia Perlis, 01000 Kangar, Perlis, Malaysia
[d] Physics Department, Center of Excellence in Renewable Energy, King Fahd University of Petroleum and Minerals,Saudi Arabia

ARTICLE INFO

Article history:
Received 19 November 2011
Received in revised form 5 January 2012
Accepted 6 January 2012
Available online 21 January 2012

Keywords:
MgO
$Mg(OH)_2$
Nanostructures
Bulk modulus
Refractive index

ABSTRACT

Two simple methods for the synthesis of $Mg(OH)_2$ nanostructures, MgO nanoflakes and MgO/$Mg(OH)_2$ nanocomposite using a conventional microwave oven are reported. The first method includes the preparation of $Mg(OH)_2$ by a simple reaction of magnesium powder with deionized water under microwave radiation. The second approach relates to the transformation of $Mg(OH)_2$ to MgO nanoflakes and grass-like nanostructures by rapid microwave hybrid heating using a SiC-based composite susceptor. The as-synthesized samples have been characterized by X-ray diffraction (XRD) and Field Emission Scanning Electron Microscope (FESEM) The optical properties of the samples are investigated using UV–visible spectroscopy to study the reflective index and optical dielectric constant.

1. Introduction

Microwave-assisted synthesis methods (MASMs) of nanomaterials have been attracting a significant attention. These methods have opened new horizons of research in materials science at the nanoscale because of many advantages over the conventional synthesis methods, such as the reduction of the time of chemical reactions, the synthesis of small particles with narrow size distribution, increased product yield rate and the synthesis of high purity materials. Moreover, MASMs are potentially more cost effective in comparison with conventional synthesis methods [1–4].

Different MASMs have been successfully used for the fast synthesis of MgO micro-and nano-structures with different morphologies including nanoparticles [5], micro and nano-structures which have different shapes such as hexahedrons, plates and others [6]. Microwave hybrid heating (MWHH) requires the use of an independent heat source such as an electric furnace (conventional heating) in combination with microwaves. A susceptor which absorbs strongly the incident microwave power can be used to reach high temperatures in a very short period of time.

MgO and $Mg(OH)_2$ nanostructures have been extensively studied. Magnesium oxide is an important non-toxic insulator material with a wide-band gap [7,8]. Additionally, MgO nanostructures have been used in the form of ultra-thin shell on the surface of some metal oxides such as SiO_2 [9], ZnO [10] and TiO_2 [11] to improve the efficiency of dye-sensitized solar cells. Magnesium hydroxide is widely used because of its non-toxicity, long-term stability and its resistivity to corrosion. Also, it is an environment-friendly material and is extensively used in many medical, industrial and agricultural products [12,13].

Up to now, several methods have been developed to synthesize $Mg(OH)_2$ and MgO nanostructures, such as the hydrothermal route [14], thermal evaporation using a horizontal tube [15,16], solvothermal reaction [17], electrochemical processes [18], precipitation technique [19], sonochemical method [20], chemical vapor transport [5], microwave-assisted synthesis method [21] and microwave plasma torch [22]. A number of researchers have used magnesium as the starting material for the preparation of magnesium oxide and magnesium hydroxide using different methods [22–27]. In ref. [5], the authors used a mixture of $Mg(NO_3)_2{\cdot}6H_2O$ with two types of fuels including sorbitol and polyethylene glycol. The mixture of magnesium nitrate and fuel dissolved in deionized water was heated in an oven at 100 °C for 3 h. In this work, a novel method involving a simpler mixture of Mg powder and

* Corresponding author at: School of Applied Physics, Faculty Science and Technology, Universiti Kebangsaan Malaysia, 43600 Bangi, Selangor, Malaysia. Tel.: +60173981135; fax: +60389269470.
** Corresponding author. Tel.: +6049775021; fax: +6049798578.
E-mail addresses: Rashad_jashani@yahoo.com (R. Al-Gaashani), yaldouri@yahoo.com (Y. Al-Douri).

0925-8388/$ – see front matter.
doi:10.1016/j.jallcom.2012.01.045

deionized water exposed to microwave to prepare $Mg(OH)_2$ nanostructures. Subsequently, MgO nanostructures were synthesized by ultra fast heating of $Mg(OH)_2$ prepared via the first method, using a SiC microwave susceptor. To best of our knowledge, this method to prepare various MgO and $Mg(OH)_2$ nanostructures is used for the first time. It is worth pointing out that the method can be used to prepare other metal hydroxides and oxides. Additionally, we studied the optical properties of refractive index and optical dielectric constant using UV–visible spectroscopy.

2. Experimental procedure

Magnesium hydroxide nanostructures were synthesized by a simple microwave-assisted method using magnesium (Mg) powder (Aldrich, Fluka). A kitchen microwave oven (Model No. EM-G430, 2.45 GHz, maximum output power 1000 W, SANYO Electric, UK) was used. In a typical experiment, 0.9 g of Mg powder and 100 mL of deionized water (resistivity 18.2 MΩ cm) were put into a 500 mL flat-bottom flask. Then, the flask containing the magnesium powder with deionized water was placed inside the oven and exposed to microwave radiations for 8 min. A hot milky solution with a white precipitate was obtained and was left after switching off the oven to cool down slowly to room temperature. Then, the white precipitate was separated by centrifugation at 4000 rpm for 10 min, washed with deionized water and acetone several times and finally dried in air at 70 °C for 20 h.

Magnesium oxide nanostructures (grass-like and nanoflakes) were synthesized by using a SiC-based susceptor. The magnesium hydroxide powder prepared as described in the previous section was divided into two equal quantities. A first half was put inside a crucible which was placed on the top of the SiC-based heater. The sample was exposed to microwaves for 2 min under air with the microwave power set at 1000 W. The second half of the powder was treated for 5 min under the same conditions. After cooling the samples down to room temperature, the white powder was easily collected as it stuck very weakly to the bottom of the crucibles. Previous measurements showed that the temperatures reached by the heater range from 1200 °C up to 1700 °C depending on the composition of the SiC-based composite and the thermal shield around the sample [28].

Finally, the structural characterization of all prepared samples was carried out by X-ray powder diffraction (XRD) using a Bruker-AXSD8 advance X-ray diffractometer with Cu–Kα radiation source (λ = 1.5418 Å). The microstructure of the samples was observed using a HITACHI S-4800 field emission scanning electron microscope (FESEM). The optical properties were analyzed by recording the (UV–vis) absorption spectra at room temperature using a Perkin-Elmer Lambda 35 spectrophotometer in the 150–1100 nm wavelength range.

3. Results and discussion

3.1. Structure and morphology of the samples

It is shown from the XRD patterns (Fig. 1) $Mg(OH)_2$ nanostructures (a), $MgO/Mg(OH)_2$ nanocomposites (b) and MgO nanoflakes (c), the sharpness of the peaks indicates that the samples were in a well crystallized form. The average crystallite sizes D of the as-prepared $Mg(OH)_2$ and MgO powder were estimated using Scherrer's formula as follows:

$$D = \frac{0.9\lambda}{\beta \cos\theta} \quad (1)$$

where λ is the X-ray wavelength of Cu–Kα radiation source (λ = 0.15418 nm), β (in radians) is the full width at half maximum (FWHM) intensity of the diffraction peak located at 2θ, and θ is the Bragg angle. The average crystallite sizes of $Mg(OH)_2$ and MgO nanoflakes were calculated to be about 43 nm and 32 nm, respectively.

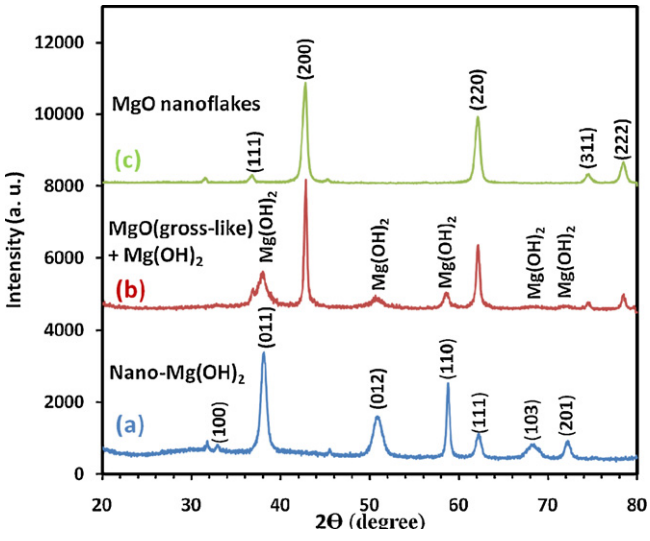

Fig. 1. XRD patterns of (a) $Mg(OH)_2$ nanostructures, (b) $MgO/Mg(OH)_2$ nanocomposites and (c) MgO nanoflakes.

Fig. 2 shows the FESEM images of the $Mg(OH)_2$ sample synthesized by the reaction of magnesium powder with deionized water under microwave exposure during 8 min with the power set at 1000 W. All the FESEM images reveal the presence of $Mg(OH)_2$ with two morphologies, namely nano-particles and nanosheets which have approximately 36–45 nm thickness (Fig. 2b).

The SEM images (a and b) of the $MgO/Mg(OH)_2$ nanocomposite prepared by thermal decomposition of $Mg(OH)_2$ under microwave hybrid heating for 2 min with the power set at 1000 W are displayed in Fig. 3. The figure shows grass-like MgO nanostructures grown on the top of $Mg(OH)_2$ sheets. The exposure time (2 min) was not enough for the complete thermal decomposition of $Mg(OH)_2$ into MgO. This was confirmed by the results obtained after 5 min treatment which showed a complete transformation of $Mg(OH)_2$ producing MgO nanoflakes of 26–44 nm thickness as displayed in SEM images Fig. 3c and d.

3.2. Growth of $Mg(OH)_2$ and MgO nanostructures

Water gradually decomposes into solvated hydrogen cations (H^+) and hydroxide anions (OH^-) under microwave heating. The degree of water dissociation increases as the temperature is increased and can be described by the following reaction [29]:

$$H_2O \leftrightarrow H^+ + OH^- \quad (2)$$

Magnesium powder is not affected by water at room temperature, but when the mixture solution (magnesium powder with deionized water) is exposed to microwave radiation, magnesium particles steadily decompose to small Mg^{2+}(aq) cations [30]. Those cations may react with hydroxide ions as follows:

$$Mg^{2+}(aq) + OH^- \leftrightarrow MgOH^+ \quad (3)$$

$$MgOH^+ + OH^- \leftrightarrow Mg(OH)_2(\text{crystalnuclei}) \quad (4)$$

$$Mg^{2+}(aq) + 2OH^- \leftrightarrow Mg(OH)_2(\text{crystalnuclei}) \quad (5)$$

According to the above possible reactions, $MgOH^+$ ions (hydroxo complexes of Mg^{2+}) act as growth unit of $Mg(OH)_2$ crystals to produce the initial $Mg(OH)_2$ nuclei (Eqs. (4) and (5)). In addition to the reasons detailed in reference [31], this is probably the main reason for the presence of two different morphologies of $Mg(OH)_2$ (nanoparticles and nanosheets, observed in Fig. 2). However, it is expected that the exposure of a solution containing different phases without stirring can lead to heterogeneities in the temperature distribution and in the viscosity of the solution. These heterogeneities can be a cause of the morphological variations observed in the case of the $Mg(OH)_2$ samples. The possible growth mechanism of the two morphologies of $Mg(OH)_2$ nanostructures prepared by simple reaction of magnesium powder with deionized water under microwave radiation during 8 min) is described in Fig. 4(a). Under microwave radiation, the obtained soluble ions (Mg^{2+}, OH^- and $MgOH^+$) polarize, aggregate and react (Eqs. (4) and (5)) to form the initial $Mg(OH)_2$ nuclei. Then, the obtained

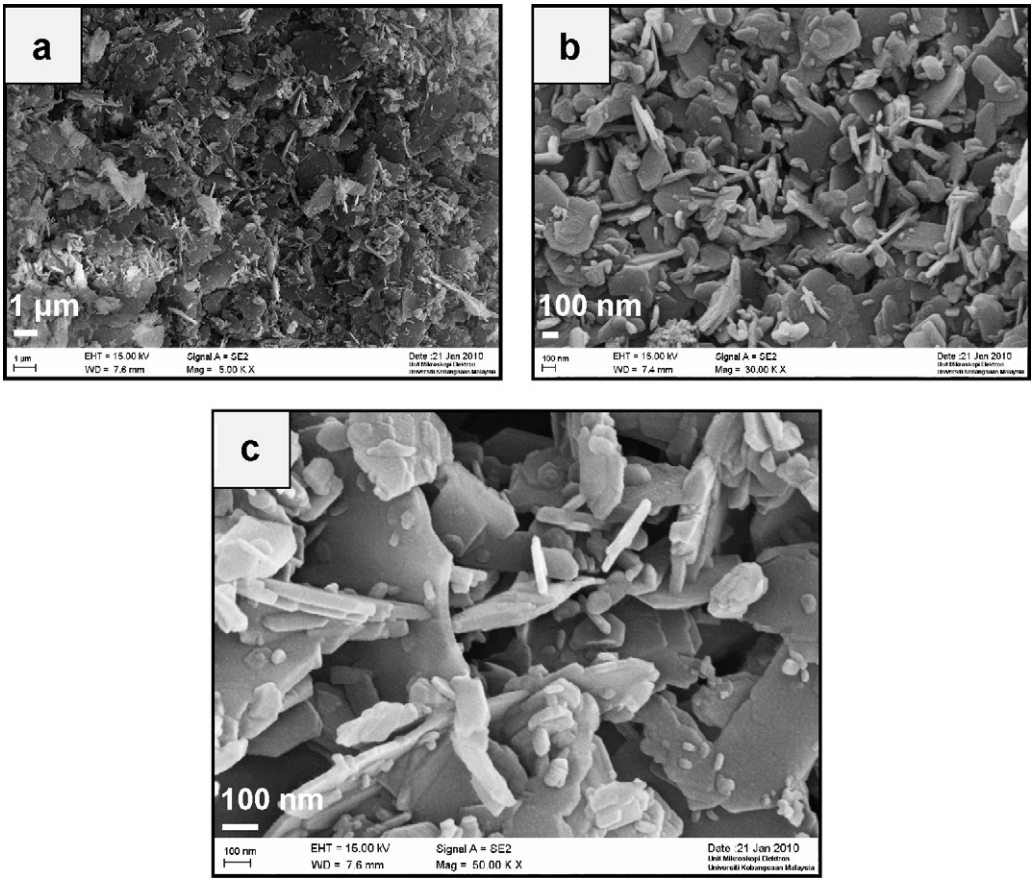

Fig. 2. FESEM images of $Mg(OH)_2$ nanostructures.

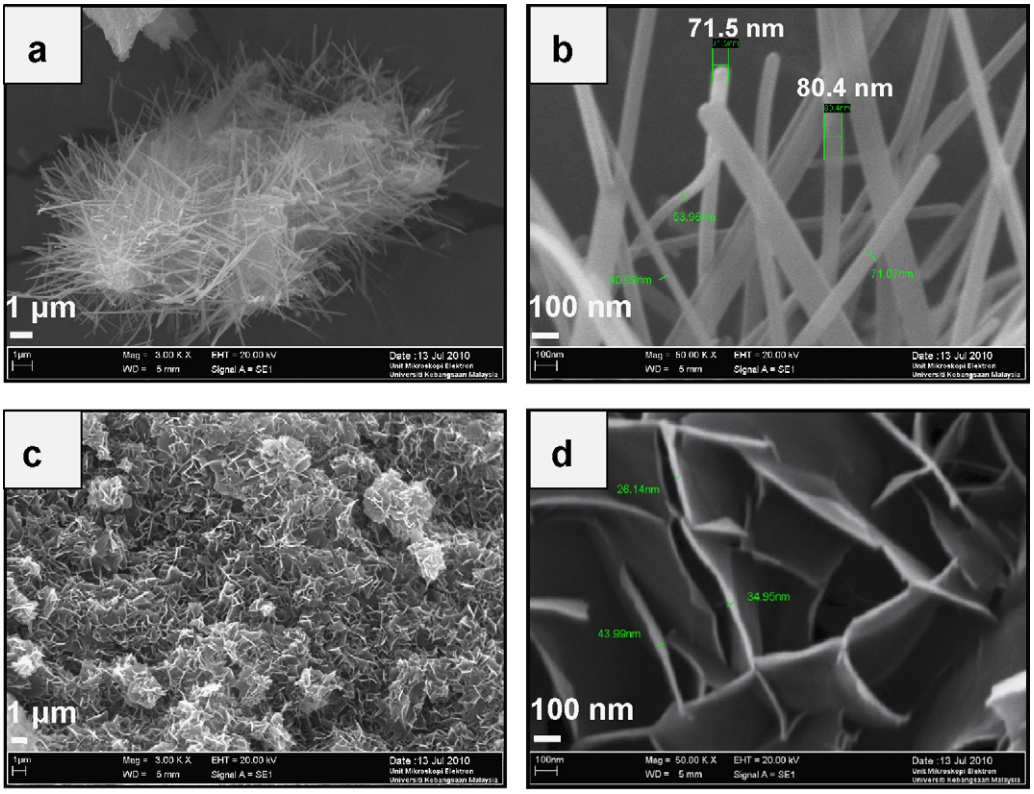

Fig. 3. SEM images of $MgO/Mg(OH)_2$ nanocomposite (grass-like (a) and (b)) and MgO nanoflakes ((c) and (d)).

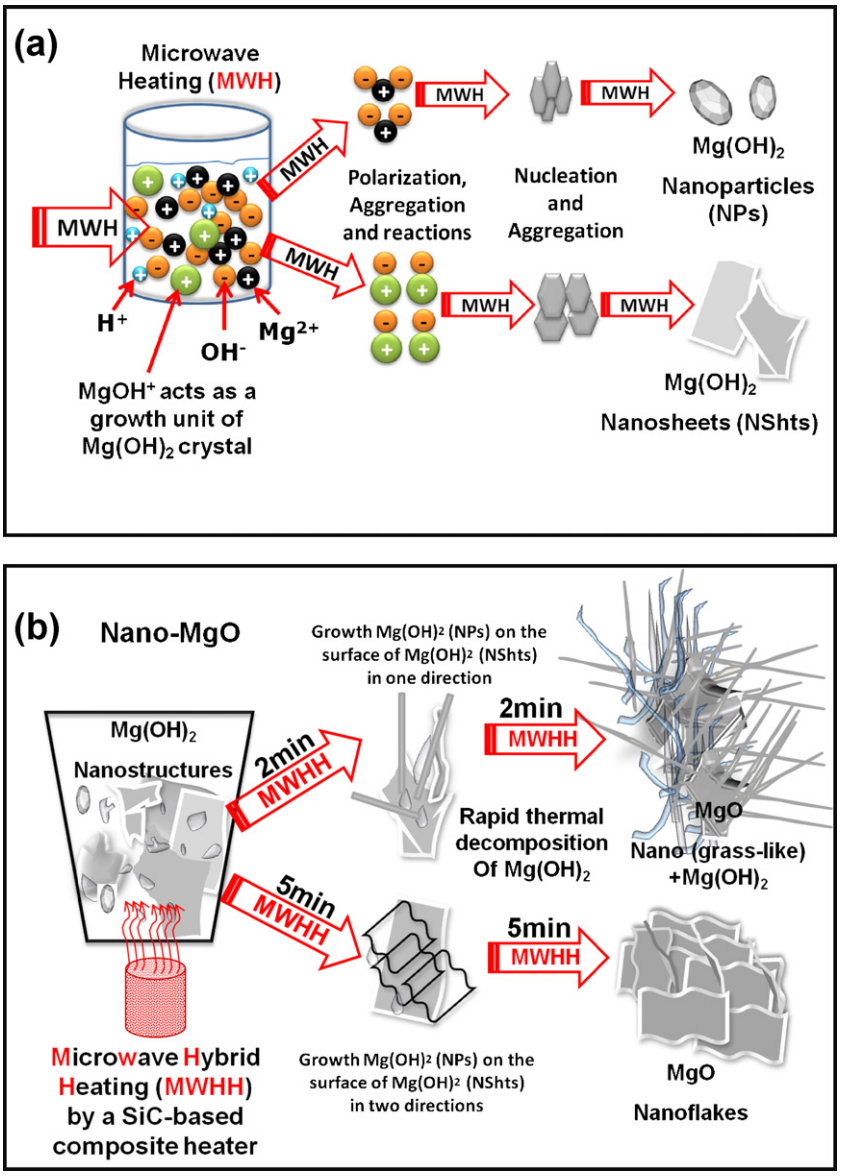

Fig. 4. The possible growth mechanism of (a) $Mg(OH)_2$ (b) MgO nanostructures synthesized by novel microwave-assisted methods.

$Mg(OH)_2$ nuclei polarize, aggregate and growth to produce $Mg(OH)_2$ nanoparticles and nanosheets as shown in Fig. 4(a).

The possible growth mechanism of grass-like MgO nanostructures on the surface of $Mg(OH)_2$ nanosheets and the production of MgO nanoflakes is shown in Fig. 4(b). For short time exposure to microwave hybrid heating (2 min) one can observe the growth of grass-like, one-dimensional MgO nanostructures on $Mg(OH)_2$ sheets. For longer exposures (5 min) only MgO nanoflakes were observed suggesting the complete decomposition of $Mg(OH)_2$ phase Fig. 4(b) as described by the following reaction:

$$Mg(OH)_2 \rightarrow MgO + H_2O \quad (6)$$

3.3. Optical properties

It is advantageous to study the optical properties of nanostructures that are important for different industrial applications. UV–vis absorption spectroscopy technique has been used to study the optical properties of many materials as powders or thin films. Experimentally, the following equation has usually been used to estimate the band gap energy E_g of various materials of direct energy gap [32].

$$(\alpha h\nu)^2 = B(h\nu - E_g) \quad (7)$$

where α is the absorption coefficient, h is Planck's constant, ν is the photon frequency, B is a material-dependent constant and E_g is the band gap energy between the conduction (CB) and valance band (VB) of the material. The value of the absorption coefficient can be determined by using the following equation [33]:

$$\alpha = \frac{-1}{d} \ln \frac{I_t}{I_0} = \frac{A}{d \log e} \approx 2.3.3 \frac{d}{A} \quad (8)$$

where d is the thickness of the used cuvette (the sample thickness), I_0 and I_t are the intensities of incident and transmitted light, respectively, A is the absorbance.

Fig. 5(a) shows the typical optical absorption spectra of (a) MgO nanoflakes (λ_{max} = 300 nm), (b) $Mg(OH)_2$ nanostructures (λ_{max} = 289 nm) and (c) $MgO/Mg(OH)_2$ nanocomposite (λ_{max} = 206 nm) respectively. In order to calculate the optical band gap energy E_g of the as-prepared $Mg(OH)_2$, MgO and $MgO/Mg(OH)_2$ nanocomposite powder, we fit the absorption data to Eq. (7) by

Table 1
Calculated refractive indices for different MgO nanostructures using Ravindra et al. [38], Herve and Vandamme [39] and Ghosh et al. [40] models corresponding to optical dielectric constant.

	n	ε_∞
$Mg(OH)_2$ nanostructure	1.878[a] 1.282[b] 1.258[c]	3.526[a] 1.643[b] 1.582[c]
MgO nanoflake	2.210[a] 1.035[b] 1.990[c] 1.736[d] 1.74[e]	4.884[a] 1.071[b] 3.960[c] 3.0[f] 3.1[g]
$MgO/Mg(OH)_2$ nanocomposite	2.192[a] 1.966[b] 1.958[c]	4.804[a] 3.865[b] 3.833[c]

[a] Ref. [38].
[b] Ref. [39].
[c] Ref. [40].
[d] Ref. [43] experimental.
[e] Ref. [44] theoretical.
[f] Ref. [45] experimental.
[g] Ref. [46] theoretical.

extrapolating of the linear region of the plot of $(\alpha h\nu)^2$ on the y-axis against photon energy ($E = h\nu$) on the x-axis. The energy gap is obtained by the x-axis intercept of the extrapolated linear part of the graph (Fig. 5(b)). The optical band gap energies of $Mg(OH)_2$ nanostructures, MgO nanoflakes and $MgO/Mg(OH)_2$ nanocomposite have been estimated to be 3.5, 3.46 and 4.5 eV respectively as shown in Fig. 5(b).

The result of MgO nanoflakes is approximately identical with that result reported by Kumari et al. [34]. It should be noted that it is not easy to obtain reliable value of E_g for MgO or $Mg(OH)_2$ because of the high hygroscopy of MgO. A thin layer of magnesium hydroxide is always present on the surface of the MgO grains when the (UV–vis) absorption spectra are recorded.

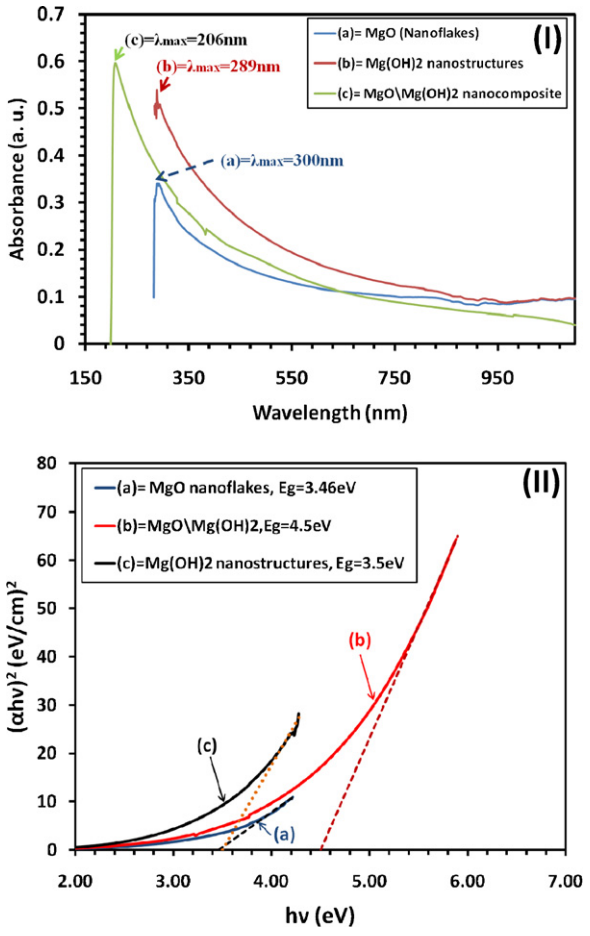

Fig. 5. UV–vis absorption spectra (i) and the estimated optical band gaps (E_g) (ii) of (a) MgO nanoflakes, (b) $MgO/Mg(OH)_2$ nanocomposites and (c) $Mg(OH)_2$ nanostructures.

The refractive index n is a very important physical parameter related to the microscopic atomic interactions. From theoretical view point, there are basically two different approaches of viewing this subject: the refractive index will be related to the density and the local polarizability of these entities [35]. Consequently, many attempts have been made in order to relate the refractive index and the energy gap E_g through simple relationships [36–38]. However, these relations of n are independent of temperature and incident photon energy. Here the various relations between n and E_g will be reviewed. Ravindra et al. [38] had been presented a linear form of n as a function of E_g:

$$n = \alpha + \beta E_g \tag{9}$$

where $\alpha = 4.048$ and $\beta = -0.62\ eV^{-1}$. Light refraction and dispersion will be inspired. Herve and Vandamme [39] proposed an empirical relation as follows:

$$n = \sqrt{1 + \left(\frac{A}{E_g + B}\right)^2} \tag{10}$$

where $A = 13.6$ eV and $B = 3.4$ eV. For group-IV semiconductors, Ghosh et al. [40] have published an empirical relationship based on the band structure and quantum dielectric considerations of Penn [41] and Van Vechten [42]:

$$n^2 - 1 = \frac{A}{(E_g + B)^2} \tag{11}$$

where $A = 8.2E_g + 134$, $B = 0.225E_g + 2.25$ and $(E_g + B)$ refers to an appropriate average energy gap of the material. The calculated refractive indices of the end-point compounds are listed in Table 1.

This is verified by the calculation of the optical dielectric constant ε_∞ which depends on the refractive index. Note that $\varepsilon_\infty = n^2$ [46]. It is clear that the investigated n using the model of Ghosh et al. [40] is important for nanostructures and nanocomposites, while Herve and Vandamme model [39] is appropriate for nanoflakes for enhancing the efficiency of dyesensitized solar cells. It means high absorption and low reflection may be attributed to increase solar cell efficiency.

4. Conclusion

We have shown that simple microwave-assisted methods can be used to produce a variety of magnesium oxide and hydroxide nanostructures for the preparation of nanostructures of other metal hydroxides and oxides. The nanostructure obtained under hybrid microwave heating is particularly interesting as it allows the massive production of uniform nanostructures as compared to other methods. The obtained results of the lattice constants and bulk moduli recommend that the used two simple methods are suitable for optoelectronics fabrication especially MgO nanoflakes and confirmed that $Mg(OH)_2$ nanostructure has the highest stiffness. It

is proved that Ghosh et al. model is recommended for nanostructures and nanocomposites, while Herve and Vandamme model is appropriate for nanoflakes to improve the photo conversion of the solar cells.

Acknowledgments

(R.A., S.R., N.T. and A.R.D.) would like to thank Universiti Kebangsaan Malaysia (UKM) for supporting this work through grant no: UKM-GUP-NBT-08-27-106 and UKM-AP-NBT-15-2010. (Y. A.) would like to acknowledge the finanicial support presented by FRGS grants numbered 9003-00249 and 9003-00255 and TWAS-Italy for the full support of his visit to JUST-Jordan under TWAS-UNESCO Associateship.

References

[1] H.M. Kingston, S.J. Haswell, Microwave-Enhanced Chemistry, American Chemical Society, Washington, DC, 1997.
[2] M. Nishioka, M. Miyakawa, H. Kataoka, H. Koda, K. Sato, T.M. Suzuki, Chem. Lett. 40 (2011) 1204.
[3] M. Nishioka, M. Miyakawa, H. Kataoka, H. Koda, K. Sato, T.M. Suzuki, Nanoscale 3 (2011) 2621.
[4] K.D. Bhatte, D.N. Sawant, R.A. Watile, B.M. Bhanage, Mater. Lett. 69 (2012) 66.
[5] E. Esmaeili, A. Khodadadi, Y. Mortazavi, J. Eur. Ceram. Soc. 29 (2009) 1061.
[6] S.H.C. Liang, I.D. Gay, J. Catal. 101 (1986) 293.
[7] P.D. Johnson, Phys. Rev. 94 (1954) 845.
[8] D.M. Roessler, W.C. Walker, Phys. Rev. 159 (1967) 733.
[9] M.K.I. Senevirathna, P.K.D.D.P. Pitigala, E.V.A. Premalal, K. Tennakone, G.R.A. Kumara, A. Konno, Sol. Energy Mater. Sol. Cells 91 (2007) 544.
[10] N.O.V. Plank, H.J. Snaith, C. Ducati, J.S. Bendall, L. Schmidt-Mende, M.E. Welland, Nanotechnology 19 (2008) 465603.
[11] B. Li, G. Lü, L. Luo, Y. Tang, J. Nat. Sci. 15 (2010) 325.
[12] J.L. Booster, A.V. Sandwihk, M.A. Reuter, Miner. Eng. 16 (2003) 273.
[13] C. Henrist, J.P. Mathieu, C. Vogels, A. Rulmont, R.J. Cloots, J. Cryst. Growth 249 (2003) 321.
[14] J. Zhang, L. Zhang, X. Peng, X. Wang, Appl. Phys. A 73 (2001) 773.
[15] Q. Yang, J. Sha, L. Wang, J. Wang, D. Yang, Mater. Sci. Eng. C 26 (2006) 1097.
[16] Y.D. Li, M. Sui, Y. Ding, G.H. Zhang, J. Zhuang, C. Wang, Adv. Mater. 12 (2000) 818.
[17] W.L. Fan, S.X. Sun, L.P. You, G.X. Cao, X.Y. Song, W.M. Zhang, H.Y. Yu, J. Mater. Chem. 13 (2003) 3062.
[18] J.P. Lv, L.Z. Qiu, B.J. Qu, J. Cryst. Growth 267 (2004) 676.
[19] M. Sugimoto, J. Magn. Chem. Mater. 133 (1994) 460.
[20] M.A. Alavi, A. Morsali, Ultrason. Sonochem. 17 (2010) 441.
[21] K.D. Bhatte, D.N. Sawant, K.M. Deshmukh, B.M. Bhanage, Particuology (2011), doi:10.1016/j.partic.2011.05.004.
[22] R. Hahn, J.G. Brunner, J. Kunze, P. Schmuki, S. Virtanen, Electrochem. Commun. 10 (2008) 288.
[23] M. Zhao, X.L. Chen, X.N. Zhang, L. Dai, J.K. Jian, Y.P. Xu, Appl. Phys. A 79 (2004) 429.
[24] H. Niu, Q. Yang, K. Tang, Y. Xie, J. Nanopart. Res. 8 (2006) 881.
[25] M.A. Shah, Q. Ahsanulhaq, J. Alloys Compd. 482 (2009) 548.
[26] N. Takahashi, Solid State Sci. 9 (2007) 722.
[27] R. Ma, Y. Bando, Chem. Phys. Lett. 370 (2003) 770.
[28] N. Tabet, R. Al Ghashani, S. Achour, Superlattices Microstruct. 45 (2009) 598.
[29] J.E. Otterstedt, D.A. Brandreth, Small Particles Technology, Plenum Publishing Corporation, 1998.
[30] M. Altmaier, V. Metz, V. Neck, R. Müller, T. Fanghnel, Geochim. Cosmochim. Acta 67 (2003) 3595.
[31] R. Al-Gaashani, S. Radiman, N. Tabet, A.R. Daud, Mater. Chem. Phys. 125 (2011) 846.
[32] J.I. Pankove, Optical Processes in Semiconductors, Dover, New York, 1970.
[33] A.D. Yoffe, Adv. Phys. 42 (1993) 173.
[34] L. Kumari, W.Z. Li, C.H. Vannoy, R.M. Leblanc, D.Z. Wan, Ceram. Int. 35 (2009) 3355.
[35] N.M. Balzaretti, J.A.H. da Jornada, Solid State Commun. 99 (1996) 943.
[36] V.P. Gupta, N.M. Ravindra, Phys. Status Solidi B 100 (1980) 715.
[37] Y. Al-Douri, A.H. Reshak, H. Baaziz, Z. Charifi, R. Khenata, S. Ahmad, U. Hashim, Solar Energy 84 (2010) 1979.
[38] N.M. Ravindra, S. Auluck, V.K. Srivastava, Phys. Status Solidi (B) 93 (1979) K155.
[39] P.J.L. Herve, L.K.J. Vandamme, J. Appl. Phys. 77 (1995) 5476.
[40] D.K. Ghosh, L.K. Samanta, G.C. Bhar, Infrared Phys. 24 (1984) 34.
[41] D.R. Penn, Phys. Rev. 128 (1962) 2093.
[42] J.A. Van Vechten, Phys. Rev. 182 (1969) 891.
[43] K. Vedam, E.D. Schmidt, Phys. Rev. 146 (1966) 548.
[44] R.E. Stephens, I.H. Malitson, J. Res. Natl. Bur. Stand. 49 (1952) 249.
[45] J.C. Phillips, Phys. Rev. 20 (1968) 550.
[46] G.A. Samara, Phys. Rev. B 27 (1983) 3494.